Atomic transition probabilities of F I spectral lines from $3s$-$3p$ and $3p$-$3d$ transition arrays

J. Musielok
Institute of Physics, Opole University, 45-052 Opole, Poland

E. Pawelec
Institute of Physics, Jagiellonian University, 30-050 Krakow, Poland

U. Griesmann and W. L. Wiese
National Institute of Standards and Technology, Gaithersburg, Maryland 20899-8420

(Received 25 November 1998)

We have measured the relative transition probabilities of about 100 $3s$-$3p$ and $3p$-$3d$ lines of neutral fluorine in the visible and near-infrared spectrum with a wall-stabilized high-current arc, which is operated under conditions very close to partial local thermodynamic equilibrium. The set of measured lines includes about 40 intersystem transitions. Our data have been placed on an absolute scale by normalizing several strong transitions to the results of the OPACITY Project calculations, which are expected to be quite accurate for such transitions. We estimate that the uncertainties of our absolute transition probability values are in the $\pm 15\%$ to $\pm 20\%$ range, while the uncertainties of the relative values do not exceed 6%, except for very weak transitions. Our results indicate that especially for $3p$-$3d$ transitions appreciable departures from *LS* coupling are encountered. Comparisons with other results indicate that earlier experimental data agree well with ours on a relative scale, but need to be renormalized. [S1050-2947(99)03408-3]

PACS number(s): 32.30.Jc, 32.70.Cs, 32.70.Fw

INTRODUCTION

The atomic transition probabilities of F I lines have been of interest mainly in connection with the analysis of SF_6 electric arcs used as high-power industrial circuit breakers. Thus, laboratory wall-stabilized arc sources have been applied to study the emissivity and other spectral properties of SF_6 plasmas. But data obtained by Schulz-Gulde and coworkers [1,2] and by Lokner, Vadla, and Vujnović [3] for prominent F I lines show marked discrepancies, and their measurements were restricted to $3s$-$3p$ transitions only. Also, lifetime data by Burshtein [4] and Delalić, Erman, and Källne [5] are not consistent, and thus make the absolute scale rather uncertain.

Extensive sets of oscillator strengths have been calculated by Kurucz and Peytremann [6] with a semiempirical approach, by Velasco, Lavin, and Martin [7] with the relativistic quantum defect orbital (RQDO) method, and by the OPACITY Project team [8] with a multiconfiguration approach. The latter calculations should establish a reliable absolute scale for the transition probabilities, but they are confined to multiplet data only. But data for fine-structure transitions, i.e., for the normally observed individual spectral lines, are of considerable interest, since appreciable departures from Russell-Saunders coupling have been observed for $3p$-$3d$ transitions for the isoelectronic spectrum of Ne II [9] and for other light atoms [10,11].

We have therefore undertaken this extended study of individual $3s$-$3p$ and $3p$-$3d$ lines, which includes numerous intersystem lines. Our results, which differ substantially from some earlier data, provide a more accurate set of atomic transition probabilities.

EXPERIMENT

We have modified a wall-stabilized arc [12] to generate fluorine spectra under reproducible, well defined conditions. Our device consists of a set of nine water-cooled copper disks with a central bore of 4 mm, forming a cylindrical wall-stabilized arc chamber with a length of 63 mm. The copper disks are separated by suitable insulator spacers. Two additional plates, incorporating the tungsten electrodes, confine the discharge volume, allowing the arc to run in a controlled atmosphere.

Figure 1(a) shows schematically the gas inlet and outlet system for three adjacent arc disks. Each disk contains chan-

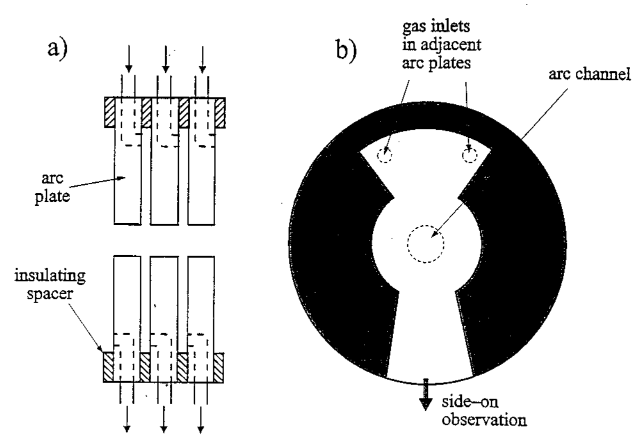

FIG. 1. (a) Schematic diagram of the gas inlet and outlet system for three adjacent arc disks. (b) The special insulating spacer made of PTFE (Teflon), with the positions of the arc channel, the gas inlet openings, and the slit for side-on observations indicated.

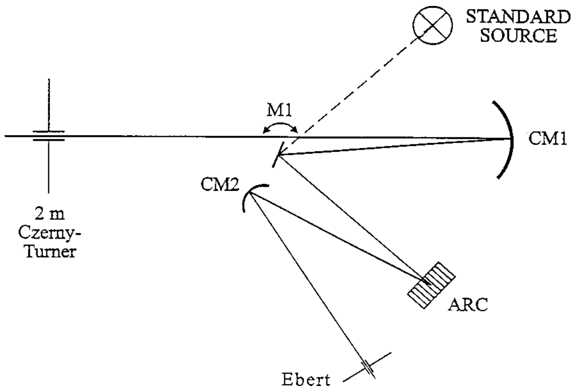

FIG. 2. Scheme of the optical arrangement.

nels, allowing gas to be introduced into and exhausted from the space between two subsequent disks. The central arc chamber was operated in helium, while the areas close to both electrodes were operated in argon in order to improve the stability of the discharge. One special insulating spacer, located between two disks in the center of the arc chamber, is made of polytetrafluorethylene (PTFE), widely known as Teflon. The shape of this spacer is shown in Fig. 1(b). Between the two disks, helium is introduced through both gas channels in the adjacent arc plates and its flow is precisely controlled by a separate needle valve and a gas flowmeter. The inlet gas channels are located on the side of the spacer opposite from the opening, where the gas is exhausted. This opening, which is in the form of a slit, also allows radiation emitted from the arc in the side-on direction to be measured. A detailed study of the emission of the fluorine spectrum emerging from this part of the arc shows that the intensity of the F I spectrum depends on (i) the arc current, (ii) the temperature of the PTFE spacer, determined by the water cooling of adjacent arc plates, and (iii) the helium gas flow rate. Over a wide range of the arc current, the intensity of the fluorine spectrum increases nearly linearly with increasing current. On the other hand, with a rising helium flow rate as well as with increased cooling of the PTFE spacer the intensity of the F I spectrum decreases. When all three parameters are fixed, very stable emission of the fluorine spectrum is achieved. These conditions (stability of the order of 1% in the line intensities) are reached after about 20 minutes of arc ignition. After that time the arc provides stable F I line emission for hours. Also, the reproducibility of the intensity of the F I spectrum is within a few percent.

Figure 2 shows schematically the optical arrangement applied for the spectroscopic measurements. The radiation either from the arc or from the standard source (tungsten strip lamp) was focused, via the plane mirror $M1$, onto the entrance slit of a 2-m Czerny-Turner monochromator by the concave mirror CM 1. The concave mirror CM 2 collected some radiation at an angle slightly off the main optical axis and imaged the arc onto the entrance slit of a 1/4-m Ebert grating monochromator.

The intensity of the fluorine emission at 6856 Å, corresponding to the F I transition $3s\ ^4P_{5/2}$–$3p\ ^4D^o_{7/2}$, was monitored during the measurements with the small Ebert monochromator to check the stability of the arc source. Spectral scans show that the signal at 6856 Å is larger than the underlying continuum by at least a factor of 8. (The exact line-to-continuum intensity ratio depends on the operating conditions of the arc.) Therefore, the monitored signal may be regarded as representing the stability of the fluorine line spectrum. Fluctuations of this intensity during experimental runs were within 1%. Each selected spectral line was measured at least four times, but the intensity measurements of a few lines, which were chosen to be the reference intensities within a set of runs, were repeated up to ten times. In order to make sure that negligible self-absorption of radiation occurs in the plasma for the studied F I lines, we have increased the fluorine emission level by a factor of 8 and repeated the measurements for the strongest F I lines. The recorded spectra show that the intensity ratios for all transitions remain constant, indicating optically thin conditions during the measuring runs. A more detailed description of the plasma source, its properties, and of the self-absorption test can be found elsewhere [11,13].

Because of the novel character of the method of fluorine excitation, we decided to check the measured branching ratios against data originating from a different light source that also emits the F I spectrum. For this comparison we utilized a microwave driven discharge in a gas mixture of argon and tetrafluoromethane (10:1) at a pressure of about 100 Pa. With this discharge we were able to achieve a sufficient population for line intensity measurements only for the $3p$ levels of F I. For the set of $3s$-$3p$ lines, studied with both light sources, the measured branching ratios were found to be the same within the experimental accuracy.

All measured F I lines exhibit the same shape, which was defined by the instrumental resolution. For all isolated lines the integrations to obtain total line intensities were done numerically, whereas for partially overlapping lines the individual contributions of blended components were obtained from the optimum fit of all line components with the known instrumental profile. The measured line intensities were then calibrated against a tungsten strip standard source calibrated at the National Institute of Standards and Technology (NIST).

PLASMA ANALYSIS

Branching ratio measurements were performed at fixed plasma conditions for each F I atomic level under consideration. Therefore, for levels with known lifetime values, knowledge of the plasma temperature is not necessary for the determination of line strengths or transition probabilities from measured line intensities. For some of the studied levels, however, the lifetimes are not available. But one may interrelate these atomic states if at least partial local thermodynamic equilibrium (PLTE) prevails in the plasma. An equilibrium criterion [14] shows that this is mainly a function of the electron density. Therefore, in order to test if the existence of PLTE is justified, the electron density of the plasma was determined from the measured full width at half maximum (FWHM) of the hydrogen H_β line. (The applied helium contained traces of hydrogen, allowing the H_β radiation to be detected.) Applying the broadening data of Vidal, Cooper, and Smith [15], an effective electron density of $2\times10^{15}\,cm^{-3}$ was determined, which is according to Griem's equilibrium criterion [14] more than a factor of 10 above the critical density required for the existence of PLTE conditions.

However, an additional validity criterion applies to inhomogeneous plasmas such as this stabilized arc source. This criterion concerns the distance over which atoms diffuse before they come into equilibrium, mainly by elastic and charge-exchange collisions. This diffusion length, for which an approximate expression is given in Ref. [14], is for our plasma conditions larger than the arc radius, mainly due to the fact that our plasma consists predominantly of helium atoms, which have small cross sections for both elastic and inelastic collisions [14]. Thus, only an average temperature across the arc radius is established, not a pronounced radial temperature distribution. Since the concept of excitation temperature becomes questionable in this case, it is necessary to avoid interrelating spectral lines with significantly different temperature dependence. Therefore, we have assembled the lines in groups with almost the same temperature dependence. In order to obtain an estimate for the ''effective'' excitation temperature of the plasma, which characterizes the population of F I excited levels, we took advantage of the fact that traces of atmospheric nitrogen are admixed into the outward plasma layers, from where also the main fluorine emission originates. From the measured relative N I line intensities, applying the Boltzmann plot method [12], an effective temperature of 9100–9800 K, depending on the helium flow, was determined. Four N I lines were selected for this purpose, at 8216.34, 7915.42, 7546.21, and 7468.31 Å, with maximum excitation energy separation exceeding 2 eV. The corresponding transition probabilities were taken from Ref. [11].

DETERMINATION OF THE ABSOLUTE SCALE OF THE TRANSITION PROBABILITIES

Radiative lifetimes for a few levels belonging to the $3p$ configuration have been determined experimentally by Burshtein [4] and Delalić, Erman, and Källne [5]. The latter authors have also measured the lifetime for the $^4D_{7/2}$ level of the $3d$ configuration. In three of the five cases where the results overlap, the differences between the two papers exceed the quoted uncertainty estimates.

In both experiments, the fluorine atoms are excited by electron beams in a nonselective manner. Burshtein used an electron beam with energies from 100 to 500 eV and Delalić, Erman, and Källne a beam at 20 keV, which are both far above the typical excitation energies for F I energy levels from 13 to 17 eV. Thus cascading, i.e., the repopulation of lower levels by electrons cascading down from higher levels, must have occurred in both experiments and is discussed in Ref. [5] to some extent. Numerous studies of this problem have shown that cascading usually causes an appreciable lengthening of the measured lifetimes [16].

The results of calculations [8] also show that a good number of the principal cascade levels have lifetimes that are comparable to or somewhat longer than the lifetimes measured by Burshtein and Delalić, Erman, and Källne [4,5]. Thus one must suspect that these lifetime measurements are significantly lengthened by cascading effects, and we therefore have not applied them to establish the absolute scale.

Instead, we have utilized the comprehensive calculations of multiplet oscillator strengths which were carried out as part of the OPACITY Project (OP) [8] for a large number of multiplets of F I with the close-coupling approximation, using the *R*-matrix code. We have done this normalization, because similar calculations carried out for the various spectra of carbon, nitrogen, and oxygen have provided very reliable results for *strong, prominent* multiplets, such as the type investigated here. Extensive comparisons with other advanced calculations and experiments—which are available for C, N, and O [17]—have shown that for these transitions the agreement of the OP data with other recent theoretical and experimental results is usually excellent, typically within $\pm 10\%$. This includes, for example, a comparison of the OP results of Yan, Taylor, and Seaton [18] with the cascade-corrected lifetimes by Reistad *et al.* [16] for C II and C III, as well as comparisons with cascade-free lifetime data for several other spectra of C, N, and O for which detailed graphical comparisons are given in Ref. [17].

TABLE I. Selected upper levels and lifetime values used for determination of the absolute scale of transition probabilities.

Line group (as defined in text)	Upper levels	Calculated lifetime (ns) [8]
(a)	$3p\ ^4S^o_{3/2}$	16.9
	$3p\ ^4P^o_{5/2}$	25.0
	$3p\ ^4D^o_{7/2,5/2,3/2}$	20.2
(b)	$3p\ ^2P^o_{3/2,1/2}$	20.0
	$3p\ ^2D^o_{5/2,3/2}$	25.9
(c)	$3d\ ^4D_{7/2}$	19.4
	$3d\ ^4F_{9/2}$	20.8

We have therefore normalized our relative data by making use of the OP results for *strong* multiplets. The selected upper levels and theoretical lifetime data are assembled in Table I.

RELATIVE TRANSITION PROBABILITY MEASUREMENTS

Because of the earlier discussed difficulty with the concept of temperature in this nonequilibrium plasma, we have carried out a nearly temperature-independent analysis. We have divided the lines into three different groups of transitions, which are normalized separately, using the respective OP results from Table I. These *line groups* originate from (a) the quartet levels of the $3p$ configuration (23 lines), (b) the doublet levels of the $3p$ configuration (17 lines), and (c) the levels (doublets and quartets) of the $3d$ configuration (71 lines). The excitation energies of the lines under study are in the range from 14.5 to 16 eV. The energy differences of the levels within each group of lines (a), (b), and (c), are, from their approximate midpoints, 0.16, 0.09, and 0.04 eV, respectively. These energy differences are thus always 1% or less of the excitation energies, and about 20% or less of the mean electron kinetic energy. We use the emission lines originating at these approximate midpoints as our reference lines, with their transition probabilities A_R from the OP calculations. We assume that other closely neighbored levels in each group of lines are populated according to a Boltzmann distribution relative to the ''OP-normalized'' level. We have

TABLE II. Measured transition probabilities (in 10^8 s^{-1}) of lines for multiplets of the $3s$-$3p$ transition array with estimated uncertainties, and comparisons with other experimental [1–3] and theoretical [6–8] results, including comparisons of the line ratios. In the first line for each *LS*-allowed multiplet, the weighted multiplet values are quoted. The OP data [8] are multiplet values only. The line data of Ref. [7] are the *LS*-coupling fractions. For the comparison of line ratios within multiplets in the second part of the table, the transition probability of the first line has been set equal to 100. The column ''*LS*'' shows the line ratios for the case of pure *LS* coupling [18]. Numbers in brackets represent powers of 10.

Term lower-upper	Wavelength (Å)	Stat. weights		Transition probabilities (10^8 s^{-1})						Ratios of transition probabilities in % for lines within multiplets				
		g_i	g_k	This expt.	Refs. [1,2]	Ref. [3]	Ref. [6]	Ref. [7]	Ref. [8]	This expt.	Expts. [1,2]	Ref. [3]	*LS* [18]	Ref. [6]
^4P-$^4S^o$	6304.2	12	4	6.58[−1]±18%	4.51[−1]	3.60[−1]	5.77[−1]	4.64[−1]	5.93[−1]					
	6239.65	6	4	2.90[−1]±18%	2.04[−1]	1.49[−1]	2.52[−1]	2.36[−1]		100	100	100	100	100
	6348.51	4	4	2.32[−1]±18%	1.62[−1]	1.39[−1]	2.03[−1]	1.53[−1]		80.0	79.4	93.3	63.4	80.6
	6413.65	2	4	1.36[−1]±18%	8.56[−2]	7.20[−2]	1.22[−1]	7.50[−2]		46.9	42.0	48.3	30.7	48.4
^2P-$^4S^o$	7298.98	4	4	2.74[−3]±19%			4.63[−3]			100				100
	7476.54	2	4	5.15[−3]±21%			3.05[−3]			188				65.9
^4P-$^4P^o$	7445.8	12	12	4.44[−1]±19%	3.11[−1]		3.68[−1]	3.21[−1]	4.10[−1]					
	7398.68	6	6	3.53[−1]±19%	2.53[−1]	1.70[−1]	3.00[−1]	2.27[−1]		100	100	100	100	100
	7482.72	4	4	6.49[−2]±18%	4.44[−2]	3.34[−2]	5.67[−2]	4.24[−2]		18.4	17.5	19.6	18.5	18.9
	7514.92	2	2	6.54[−2]±19%	4.12[−2]		4.38[−2]	5.27[−2]		18.5	16.3		22.8	14.6
	7331.96	6	4	2.42[−1]±19%	1.72[−1]	1.26[−1]	2.09[−1]	1.49[−1]		68.6	68.0	74.1	66.3	70.0
	7425.64	4	2	3.93[−1]±19%	2.63[−1]	1.90[−1]	3.25[−1]	2.70[−1]		111	104	112	118	108
	7552.23	4	6	8.90[−2]±18%	6.02[−2]	4.63[−2]	6.92[−2]	9.31[−2]		25.2	23.8	27.2	40.4	23.1
	7573.39	2	4	1.32[−1]±19%	9.35[−2]	6.17[−2]	1.01[−1]	1.29[−1]		37.4	37.0	36.3	55.4	33.7
^2P-$^4P^o$	9016.85	2	2	2.33[−2]±20%										
^4P-$^4D^o$	6859.0	12	20	4.62[−1]±18%	3.54[−1]	3.10[−1]	4.63[−1]	3.89[−1]	4.94[−1]					
	6856.03	6	8	4.87[−1]±18%	3.42[−1]	3.42[−1]	4.67[−1]	3.88[−1]		100	100	100	100	100
	6902.47	4	6	3.51[−1]±18%	2.72[−1]	2.13[−1]	3.61[−1]	2.69[−1]		72.1	79.5	69.6	68.6	77.3
	6909.81	2	4	2.07[−1]±18%	1.73[−1]	1.46[−1]	2.26[−1]	1.61[−1]		42.5	50.6	47.7	40.7	48.4
	6773.98	6	6	9.55[−2]±18%	8.08[−2]	7.71[−2]	9.21[−2]	1.20[−1]		19.6	23.6	25.2	31.2	19.7
	6834.26	4	4	2.18[−1]±18%	1.90[−1]	1.70[−1]	2.31[−1]	2.10[−1]		44.8	55.6	55.6	53.8	49.5
	6870.22	2	2	4.01[−1]±18%	3.18[−1]	2.85[−1]	4.16[−1]	3.25[−1]		82.3	93.0	91.9	82.8	89.1
	6708.27	6	4	1.09[−2]±18%	9.50[−3]	1.28[−2]	8.88[−3]	2.05[−2]		2.2	2.8	4.2	5.3	1.9
	6795.52	4	2	5.89[−2]±18%	5.23[−2]	6.17[−2]	5.87[−2]	6.64[−2]		12.1	15.3	20.2	17.1	12.6
^2P-$^4D^o$	8040.03	4	6	1.43[−2]±18%			1.04[−2]			100				100
	8159.51	2	4	3.29[−3]±18%			2.63[−3]			23.0				25.3
^2P-$^2S^o$	7369.4	6	2	5.04[−1]±18%	3.43[−1]	2.46[−1]	4.25[−1]	2.39[−1]	4.32[−1]					
	7311.02	4	2	4.50[−1]±18%	2.98[−1]	2.13[−1]	3.85[−1]	2.36[−1]		100	100	100	100	100
	7489.14	2	2	5.48[−2]±18%	4.60[−2]	3.34[−2]	4.02[−2]	1.13[−1]		12.2	15.4	15.7	46.4	10.4
^2P-$^2P^o$	7067.4	6	6	5.71[−1]±19%	3.74[−1]		4.59[−1]	3.82[−1]	5.01[−1]					
	7037.46	4	4	4.23[−1]±19%	2.83[−1]	2.93[−1]	3.37[−1]	3.20[−1]		100	100	100	100	100
	7127.89	2	2	5.03[−1]±18%	3.37[−1]	2.57[−1]	4.14[−1]	2.51[−1]		119	119	87.7	77.1	123
	6966.35	4	2	6.64[−2]±20%	6.18[−2]		4.54[−2]	1.31[−1]		15.7	21.8		41.1	13.5
	7202.36	2	4	1.49[−1]±18%	7.92[−2]	6.68[−2]	1.22[−1]	6.14[−2]		35.2	28.0	22.8	18.7	36.2

TABLE II. *(Continued).*

Term lower-upper	Wavelength (Å)	Stat. weights		Transition probabilities (10^8 s^{-1})						Ratios of transition probabilities in % for lines within multiplets				
		g_i	g_k	This expt.	Refs. [1,2]	Ref. [3]	Ref. [6]	Ref. [7]	Ref. [8]	This expt.	Expts. [1,2]	Ref. [3]	*LS* [18]	Ref. [6]
^4P-$^2P^o$	6047.54	6	4	2.36[−3]±21%	2.86[−3]	2.31[−3]	4.67[−3]			100	100	100		100
	6149.76	4	4	1.90[−3]±19%	1.33[−3]	1.28[−3]	4.31[−3]			80.5	46.5	55.4		92.3
	6210.87	2	4	9.15[−4]±20%	7.61[−4]	7.71[−4]	2.12[−3]			38.7	26.6	33.4		45.4
^2P-$^2D^o$	7759.8	6	10	3.30[−1]±18%	2.26[−1]	1.86[−1]	3.58[−1]	3.10[−1]	3.86[−1]					
	7754.69	4	6	3.23[−1]±18%	2.18[−1]	1.77[−1]	3.52[−1]	3.09[−1]		100	100	100	100	100
	7800.21	2	4	2.52[−1]±18%	1.68[−1]	1.36[−1]	2.62[−1]	2.57[−1]		78.0	77.1	76.8	81.9	74.4
	7607.17	4	4	8.95[−2]±18%	6.82[−2]	6.42[−2]	1.05[−1]	5.39[−1]		27.7	31.3	36.3	17.7	29.8
^4P-$^2D^o$	6569.69	6	6	3.86[−3]±18%	3.65[−3]	2.83[−3]	2.29[−3]			100	100	100		100
	6690.48	4	6	1.46[−2]±19%	1.44[−2]	1.16[−2]	1.27[−2]			378	395	410		555
	6463.50	6	4	3.97[−4]±20%			3.64[−4]			10.3				15.9
	6580.39	4	4	2.51[−3]±18%	2.06[−3]	2.31[−3]	2.02[−3]			65.0	56.4	81.6		88.2
	6650.40	2	4	3.49[−3]±18%	3.65[−3]	3.08[−3]	3.68[−3]			90.4	100	109		161

measured the intensity ratios I_x/I_R of various lines x against these few OP-reference lines R, and apply the PLTE relation [11]

$$\frac{A_x}{A_R}=\frac{I_x\lambda_x g_R}{I_R\lambda_R g_x}\exp\frac{E_x-E_R}{kT} \tag{1}$$

to obtain the transition probabilities A_x. λ and g are the known wavelengths and statistical weights, respectively. T is the earlier estimated average temperature, and we emphasize again that the energy differences E_x-E_R have been minimized to achieve nearly temperature-independent conditions.

The uncertainties of our measurements have been calculated taking into account all pertinent contributions as listed in a previous paper [11], where a technique very similar to the present work was applied. The uncertainties given in the tables are one-standard deviations, obtained from the root of the sum of the squares of the component deviations (RSS) including the uncertainties of relative line intensity measurements, uncertainties of the temperature determination, and the possible influence of self-absorption effects. Also included are the relative uncertainties for the OP results [8], which are estimated to be ±10% for those strong lines which we utilized for the normalization of our data.

RESULTS AND DISCUSSION

In Table II, our transition probabilities for lines originating from levels of the $3p$ configuration are compared with other experimental results [1–3], with the OPACITY Project data [8], with the RQDO calculations [7]—where the determination of A_{ki} values for the individual lines is based on the *LS* coupling fractions [19]—and with the results of semiempirical calculations of Kurucz and Peytremann [6]. The data quoted in the sixth column of Table II are obtained by multiplying the original data of Baruschka and Schulz-Gulde [1] by a factor of 1.2, as suggested by Schulz-Gulde and Wenzel [2] in a later paper. We do not compare our results with those of Vujnović and Burshtein [20], because their data are renormalized results of Ref. [1]. In Table III our transition probabilities of *LS*-allowed lines of the $3p$-$3d$ transition array are compared with the OP multiplet data [8], with the RQDO results [7], and with results of the semiempirical calculations of Kurucz and Peytremann [6]. In Fig. 3 and Table IV, results for intersystem transitions of the $3p$-$3d$ transition array are compared with the calculations of Kurucz and Peytremann [6]. For the $3s$-$3p$ transition array, the best agreement is found with the data of Baruschka and Schulz-Gulde [1] after applying the correction suggested by Schulz-Gulde and Wenzel [2]. On average our transition probabilities are about 30% larger. Also, the transition probabilities of Lokner, Vadla, and Vujnović [3] are systematically smaller than ours (by a factor of 0.67).

While some of our results are directly normalized to the respective OPACITY Project data, numerous differences with OP data show up for other multiplets. Departures from the *LS*-coupling scheme result in significant discrepancies between A_{ki} values for weaker fine-structure components obtained by Velasco, Lavin, and Martin [7] and those determined in this work. The multiplet data of Ref. [7] are sys-

TABLE III. Measured transition probabilities (in $10^8\ s^{-1}$) of lines for multiplets of the $3p$-$3d$ transition array with estimated uncertainties, and comparison with the semiempirical calculations by Kurucz and Peytremann (KP) [6], the RQDO results [7], and the OP data [8]. In the first line for each multiplet, the weighted values are given for the experiment, the RQDO data, and for KP. In the OP calculations, only the multiplet values have been determined. The data for individual lines in Ref. [7] are the *LS*-coupling fractions. Numbers in brackets represent powers of 10.

Term lower-upper	Wavelength (Å)	Stat. weights		Transition probabilities ($10^8\ s^{-1}$)				Ratios of transition probabilities in % within multiplets		
		g_i	g_k	This expt.	Ref. [6]	Ref. [7]	Ref. [8]	This expt.	*LS*	Ref. [6]
$^4D^o$-^4F	8 862.6	20	28	3.20[−1] ± 18%	3.32[−1]	6.01[−1]	4.81[−1]			
	8 900.90	8	10	4.64[−1] ± 18%	4.52[−1]	5.90[−1]		100	100	100
	8 807.58	6	8	2.05[−1] ± 18%	2.25[−1]	5.24[−1]		44.2	88.4	49.8
	8 912.76	4	6	2.19[−1] ± 18%	2.43[−1]	4.47[−1]		47.2	74.7	53.8
	8 910.23	2	4	1.98[−1] ± 18%	2.25[−1]	4.21[−1]		42.7	69.7	49.8
	8 672.63	8	8	5.61[−3] ± 18%	6.23[−3]	8.99[−2]		1.2	15.4	1.4
	8 799.36	6	6	4.06[−2] ± 18%	3.14[−2]	1.49[−1]		8.8	25.3	6.9
	8 844.50	4	4	7.31[−2] ± 18%	8.89[−2]	1.71[−1]		15.8	28.4	19.7
	8 664.66	8	6		3.64[−4]	6.04[−3]			1.0	0.081
	8 732.82	6	4		2.64[−3]	1.25[−2]			2.1	0.58
$^4P^o$-^4D	8 263.2	12	20	3.34[−1] ± 18%	3.38[−1]	5.06[−1]	4.02[−1]			
	8 230.77	6	8	3.79[−1] ± 18%	3.39[−1]	5.09[−1]		100	100	100
	8 298.58	4	6	1.60[−1] ± 18%	1.65[−1]	3.51[−1]		42.2	68.3	48.7
	8 345.55	2	4	6.06[−2] ± 18%	6.15[−2]	2.07[−1]		16.0	40.0	18.1
	8 214.72	6	6	1.48[−1] ± 18%	1.77[−1]	1.53[−1]		39.1	30.2	52.2
	8 274.61	4	4	1.95[−1] ± 21%	2.07[−1]	2.69[−1]		51.5	52.6	61.1
	8 302.39	2	2	1.94[−1] ± 19%	2.02[−1]	4.20[−1]		51.2	81.1	59.6
	8 191.24	6	4	4.26[−2] ± 19%	4.85[−2]	2.58[−2]		11.2	5.1	14.3
	8 232.18	4	2	1.08[−1] ± 18%	1.63[−1]	8.52[−2]		28.5	16.7	48.1
$^4D^o$-^4D	9 130.0	20	20		1.09[−1]	1.39[−1]	1.13[−1]			
	9 025.47	8	8	1.43[−1] ± 18%	1.35[−1]	1.22[−1]		100	100	100
	9 151.80	6	6	1.04[−1] ± 18%	8.00[−2]	7.98[−2]		72.7	64.1	59.3
	9 244.60	4	4	5.26[−2] ± 18%	4.37[−2]	5.45[−2]		36.8	43.4	32.4
	9 262.69	2	2		2.45[−2]	6.80[−2]			54.0	18.1
	9 006.18	8	6	2.85[−2] ± 19%	2.86[−2]	2.72[−2]		19.9	22.3	21.2
	9 122.66	6	4		3.65[−2]	4.89[−2]			39.5	27.0
	9 191.67	4	2		3.86[−2]	6.92[−2]			55.2	28.6
	9 171.72	6	8			1.97[−2]			15.8	
	9 274.52	4	6		3.73[−4]	3.15[−2]			25.1	0.28
	9 316.44	2	4		4.72[−5]	3.35[−2]			26.5	0.035
$^4S^o$-^4P	9 892.3	4	12	1.27[−1] ± 24%	1.16[−1]	2.71[−1]	2.12[−1]			
	9 822.16	4	6	1.52[−1] ± 24%	9.81[−2]	2.76[−1]		100	100	100
	9 902.73	4	4	9.82[−2] ± 18%	1.32[−1]	2.70[−1]		64.6	97.2	135
	10 087.1	4	2	1.08[−1] ± 18%	1.40[−1]	2.57[−1]		71.1	92.2	143
$^4P^o$-^4P	7 973.9	12	12	1.18[−1] ± 18%	1.35[−1]	2.64[−1]	2.54[−1]			
	7 879.18	6	6	3.56[−2] ± 18%	3.66[−2]	2.19[−1]		100	100	100
	8 009.08	4	4		1.11[−3]	4.03[−2]			18.2	3.0
	8 197.73	2	2	3.32[−2] ± 18%	5.70[−2]	4.80[−2]		93.3	21.1	156
	7 930.95	6	4	2.90[−2] ± 18%	3.42[−2]	1.39[−1]		81.5	62.7	93.4
	8 129.27	4	2	1.29[−1] ± 19%	1.39[−1]	2.44[−1]		362	108	380
	7 956.29	4	6	3.29[−2] ± 18%	4.12[−2]	9.22[−2]		92.4	41.5	113
	8 075.52	2	4	1.41[−1] ± 18%	1.54[−1]	1.24[−1]		396	55.1	421

TABLE III. *(Continued).*

Term lower-upper	Wavelength (Å)	Stat. weights g_i	g_k	Transition probabilities (10^8 s^{-1}) This expt.	Ref. [6]	Ref. [7]	Ref. [8]	Ratios of transition probabilities in % within multiplets This expt.	LS	Ref. [6]
$^4D^o$-^4P	8 778.1	20	12		4.87[−2]	1.71[−2]	8.93[−3]			
	8 604.45	8	6	8.49[−4] ± 20%	5.58[−4]	1.43[−2]		100	100	100
	8 800.97	6	4		6.50[−4]	1.07[−2]			73.6	116
	9 063.56	4	2		1.12[−4]	7.96[−3]			53.4	20.1
	8 737.27	6	6	2.74[−2] ± 20%	4.01[−2]	3.15[−3]		3230	21.5	7190
	8 914.40	4	4	5.36[−3] ± 24%	1.42[−2]	5.29[−3]		631	36.0	2540
	9 132.61	2	2		7.28[−3]	7.84[−3]			52.2	1300
	8 849.06	4	6	3.05[−2] ± 18%	3.41[−2]	3.41[−4]		3590	2.3	6110
	8 981.19	2	4	1.23[−2] ± 18%	1.53[−2]	8.27[−4]		1450	5.5	2740
$^1D^o$-^2F	9 341.4	10	14	1.79[−1] ± 18%	1.80[−1]		4.40[−1]			
	9 433.65	6	8	2.35[−1] ± 18%	2.25[−1]			100	100	100
	9 235.37	4	6	1.04[−1] ± 18%	1.19[−1]			44.3	99.5	52.9
	9 026.89	6	6		2.79[−5]				7.6	0.012
$^2P^o$-^2D	10 882.0	6	10		1.20[−1]	2.92[−1]	2.48[−1]			
	10 862.2	4	6	1.33[−1] ± 20%	1.36[−1]	2.94[−1]		100	100	100
	10 940.3	2	4		5.18[−2]	2.40[−1]			81.6	38.1
	10 769.4	4	4		4.34[−2]	5.03[−2]			17.1	31.9
$^2D^o$-^2D	9 567.4	10	10		1.02[−1]	1.27[−1]	1.04[−1]			
	9 505.30	6	6	8.23[−2] ± 20%	8.91[−2]	1.21[−1]		100	100	100
	9 662.07	4	4	4.49[−2] ± 18%	6.19[−2]	1.11[−1]		54.6	91.8	69.5
	9 434.12	6	4		1.36[−2]	1.32[−2]			10.9	15.3
	9 736.74	4	6	2.73[−2] ± 19%	3.01[−2]	8.04[−3]		33.2	6.6	33.8
$^2S^o$-^2P	9 760.1	2	6	6.56[−2] ± 33%	9.59[−2]	2.80[−1]	2.20[−1]			
	9 699.46	2	4	6.37[−2] ± 35%	5.23[−2]	2.85[−1]		100	100	100
	9 883.65	2	2	6.92[−2] ± 26%	1.83[−1]	2.71[−1]		109	94.6	350
$^2P^o$-^2P	10 346.0	6	6		1.37[−1]	1.67[−1]	1.69[−1]			
	10 226.9	4	4		4.19[−2]	1.60[−1]			100	100
	10 592.1	2	2		1.83[−2]	1.18[−1]			72.4	43.7
	10 431.8	4	2		3.44[−2]	6.07[−2]			37.8	82.1
	10 380.9	2	4	1.02[−1] ± 18%	1.38[−1]	3.12[−2]			19.2	329

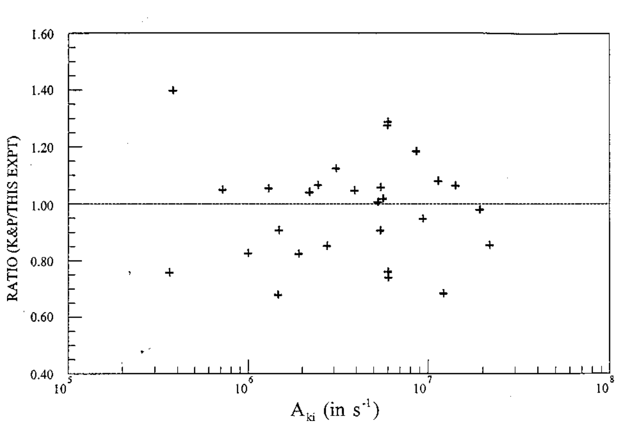

FIG. 3. Transition probability ratios [(Ref. [6])/(Expt.)] for intersystem lines of the $3p$-$3d$ transition array versus our measured data.

tematically smaller than those of Ref. [8], and therefore also ours.

In the case of the $3p$-$3d$ transition array only comparisons with calculated data are possible. The results of Ref. [7], in contrast to the $3s$-$3p$ transition array, are systematically larger than the OP results [8], typically by about 25%, with the exception of the multiplet $^4P^o$-^4P, where both theories agree well, and the multiplet $^4D^o$-^4P, where the discrepancy reaches nearly a factor of 2. The agreement between our results and those provided by these recent theoretical approaches is rather unsatisfactory. For the multiplet data, discrepancies of about 50–100 % are encountered, and discrepancies for individual lines are sometimes very large. For example, in the case of the $^4D^o$-^4P multiplet the fine-structure component which according to the LS-coupling scheme should be the strongest within the multiplet is the weakest one measured in our experiment.

TABLE IV. Measured transition probabilities (in $10^8\ s^{-1}$) of intersystem transitions belonging to the $3p$-$3d$ transition array, including uncertainties, and comparison with semiempirical results of Kurucz and Peytremann [6]. Numbers in brackets represent powers of 10.

Term Lower-upper	Wavelength (Å)	Statistical weights		Transition probabilities in $10^8\ s^{-1}$	
		g_i	g_k	This expt.	Ref. [6]
$^4P^o$-^4F	7 936.31	6	8	2.76[−2] ± 18%	2.35[−2]
$^2D^o$-^4F	9 178.68	6	8	1.93[−1] ± 18%	1.89[−1]
	9 384.96	4	6	5.97[−2] ± 18%	7.61[−2]
$^2P^o$-^4F	10 426.29	4	6	5.65[−2] ± 18%	5.75[−2]
$^2S^o$-^4F	9 794.80	2	4	6.05[−2] ± 18%	4.47[−2]
$^4D^o$-^2F	9 042.10	6	8	2.18[−1] ± 18%	1.86[−1]
	8 777.73	4	6	6.02[−2] ± 18%	7.75[−2]
$^4S^o$-^2F	9 734.34	4	6	9.39[−2] ± 18%	8.89[−2]
$^4P^o$-^2F	7 822.59	6	6	1.92[−2] ± 18%	1.58[−2]
	7 898.56	4	6	1.22[−1] ± 20%	8.33[−2]
$^2D^o$-^4D	9 574.80	6	8	1.47[−2] ± 18%	9.97[−3]
$^4S^o$-^2D	10 293.01	4	6	3.09[−2] ± 18%	3.47[−2]
	10 209.57	4	4	5.46[−2] ± 20%	4.94[−2]
$^4P^o$-^2D	8 179.34	6	6	6.03[−2] ± 21%	4.58[−2]
	8 126.56	6	4	3.92[−2] ± 18%	4.10[−2]
	8 208.63	4	4	5.49[−2] ± 20%	5.80[−2]
$^4D^o$-^2D	8 963.66	8	6	3.61[−3] ± 40%	2.73[−3]
	9 232.85	2	4	1.49[−2] ± 19%	1.35[−2]
$^2S^o$-^2D	10 186.15	2	4	5.29[−2] ± 18%	5.32[−2]
$^2D^o$-^4P	9 102.33	6	6	2.46[−2] ± 18%	2.62[−2]
	9 314.34	4	6	1.42[−1] ± 18%	1.51[−2]
$^4S^o$-^2P	9 720.57	4	4	7.18[−3] ± 26%	7.53[−3]
$^4P^o$-^2P	7 954.09	2	4	2.20[−2] ± 18%	2.29[−2]
	8 077.52	2	2	1.14[−1] ± 18%	1.23[−1]
$^4D^o$-^2P	8 766.61	4	4	1.00[−2] ± 20%	8.25[−3]
	8 831.23	2	4	8.62[−2] ± 18%	1.02[−1]
	8 916.89	4	2	3.78[−3] ± 21%	5.28[−3]
	8 983.65	2	2	1.30[−2] ± 19%	1.37[−2]

We have also tested another normalization procedure, where the absolute scale is established by fitting some of our relative multiplet A_{ki} values to the OP data. This normalization has been performed again for each line group (a)–(c) separately and by utilizing only the results for the very strong multiplets. In the case of the $3s$-$3p$ transition array the absolute scales for both groups (*a*) and (*b*) differ only by about 3.5% from those based on lifetimes for the selected levels listed in Table I. However, in the case of the $3p$-$3d$ transitions the normalization to strong multiplets leads to significant overestimates of the A_{ki} values for the strongest individual fine-structure components. The transition probability for the only line originating from the level $3d\ ^4F_{9/2}$ yields in this scale a lifetime value of 12 ns instead of 20.8 ns resulting from the OP data. Similarly, for the level $3d\ ^4D_{7/2}$, the resulting lifetime would be 10.3 ns, instead of 19.4 ns.

Our experience for similar cases with large departures from *LS* coupling has been that good agreement for the strongest lines is most important. Therefore, we decided to rely on the scale based on calculated lifetime values, presented in Table I.

The overall agreement between our data and the results of the semiempirical calculations of Kurucz and Peytremann [6] is satisfactory. More than 75% of their results for the intersystem lines of the $3p$-$3d$ transition array agree with our measurements within the uncertainties of our experiment. For the *LS*-allowed $3p$-$3d$ transitions, about 60% of the Kurucz and Peytremann results agree with our data within the uncertainties of our experiment.

ACKNOWLEDGMENTS

Two of the authors (J.M. and E.P.) were supported in part by the M. Sklodowska-Curie Foundation under Project No. MEN-NIST-96-260. The work of J.M. and E.P. was performed at the National Institute of Standards and Technology.

[1] G. Baruschka and E. Schulz-Gulde, Astron. Astrophys. **44**, 335 (1975).
[2] E. Schulz-Gulde and A. Wenzel, J. Phys. B **13**, 3733 (1980).
[3] V. Lokner, Z. Vadla, and V. Vujnović, J. Quant. Spectrosc. Radiat. Transf. **30**, 187 (1983).
[4] M. I. Burshtein, Opt. Spektrosk. **55**, 775 (1983) [Opt. Spectrosc. **55**, 464 (1983)].
[5] Z. Delalić, P. Erman, and E. Källne, Z. Phys. D **17**, 87 (1990).
[6] R. L. Kurucz and E. Peytremann, Smithson. Astrophys. Obs. Spec. Rep. **362**, (1975).
[7] A. M. Velasco, C. Lavin, and I. Martin, J. Quant. Spectrosc. Radiat. Transf. **57**, 509 (1997).
[8] W. Cunto and C. Mendoza, Rev. Mex. Astron. Astrofis. **23**, 107 (1992).
[9] U. Griesmann, J. Musielok, and W. Wiese, J. Opt. Soc. Am. B **14**, 2204 (1997).
[10] J. Musielok, G. Veres, and W. L. Wiese, J. Quant. Spectrosc. Radiat. Transf. **57**, 395 (1997).
[11] J. Musielok, W. L. Wiese, and G. Veres, Phys. Rev. A **51**, 3588 (1995).
[12] W. L. Wiese, in *Methods of Experimental Physics*, edited by B. Bederson and W. L. Fite (Academic, New York, 1968), Vol. 7B, pp. 307–353.
[13] J. Musielok and E. Pawelec, Zesz. Nauk. Uniw. Opole, Fiz. **27**, 185 (1997).
[14] H. R. Griem, *Plasma Spectroscopy* (McGraw-Hill, New York, 1964).
[15] C. R. Vidal, J. Cooper, and E. W. Smith, Astrophys. J., Suppl. **25**, 37 (1973).
[16] See, for example, N. Reistad, R. Hutton, A. E. Nilsson, I. Martinson, and S. Mannervik, Phys. Scr. **34**, 151 (1986).
[17] W. L. Wiese, J. R. Fuhr, and T. M. Deters, J. Phys. Chem. Ref. Data, Monogr. **7**, (1996).
[18] Yu Yan, K. T. Taylor, and M. J. Seaton, J. Phys. B **20**, 6399 (1987).
[19] C. W. Allen, *Astrophysical Quantities*, 3rd ed. (Athlone, London, 1973).
[20] V. Vujnović and M. L. Burshtein, Astron. Astrophys. **151**, 442 (1985).